Directionally Controllable Squeeze Film Damper Using Liquid Crystal

Young-Kong Ahn*, Shin Morishita* and Bo-Suk Yang**

(Received February 11, 1998)

Liquid crystals (LC) are characterized by its phase, which appears as an intermediate state between crystalline solid and isotropic liquid. This intermediate phase is caused by orientation of molecules, and it can be controlled by an externally applied electric or magnetic field. Subjected to an electric field, the viscosity of the LC varies according to the applied electric field strength, which is called the electroviscous effect. This paper describes an application study of the electroviscous effect of a LC to a controllable squeeze film damper (SFD) for a rotating machine. A prototype controllable SFD using a LC was constructed and its performance was studied. It should be noted that the present SFD can produce anisotropic damping force for a flexible rotor at the supporting position, which enables us to stabilize a flexible rotor in a wide range of its rotating speed.

Key Words: Squeeze Film Damper, Liquid Crystal, Electro-Rheological Fluid (ER Fluid), ER Effect, Directional Damping, Electric Field, Flexible Rotor

1. Introduction

Electro-Rheological (ER) fluid is known as one of highly functional fluids whose apparent viscosity can be varied by the externally applied electric field strength. It is generally classified into two groups; one is a colloidal suspension and the other is a homogeneous liquid. In the former type of the ER fluid, i. e. colloidal suspension, the applied electric field causes the variation of yield stress of the fluid, the property of which can be described by the Bingham plastic model. ER fluid of the latter type is known as a liquid crystal (LC), the Newtonian viscosity can be varied by the applied electric or magnetic field strength. The attractive characteristics of the ER fluid, wide variation of its apparent viscosity, controllability and quick response time, lead to make various attempt of applying the dispersion type ER fluid (Morishita and Ura, 1993) to mechanical equipments such as clutches, brakes, hydraulic valves, engine mounts and semi-active dampers.

In addition, LC has been applied as a lubricant in tribological field for better lubricating condition (Cognard, J., 1990) and estimated theoretically characteristics of LC as a lubricant (Fischer et al., 1988 ; Ticky and Rhim, 1989). Moreover, LC has a characteristics of which its viscosity can be widely changed by an externally applied electric field (Morishita, Nakano and Kimura, 1993 ; Honda, Kurosawa and Sasada, 1979). It is thought that a LC is a useful material in the mechanical engineering fields (Morishita, 1995).

A squeeze film damper (SFD) has been widely used as a damping equipment of rotating systems, and viscosity of lubricating oil and the radial clearance of the damper govern its damping characteristics. The existence of supporting optimum damping forces for every whirling mode of a flexible rotor has been pointed out (Satio, Someya and Azuma, 1982). A controllable SFD using dispersion type ER fluid was early constructed (Morishita and Mitsui, 1992) and

* Department of Mechanical Engineering, Yokohama National University, 156 Tokowadai, Hodogaya-ku, Yokohama 240, Japan

** School of Mechanical & Automotive Engineering, Pukyong National University, 599 Daeyon-dong, Nam-ku, Pusan 608-737, Korea

showed the controllability of the supporting damping by applying the electric field.

This paper describes a controllable SFD that uses LC as a lubricant which can produce anisotropic damping forces in the horizontal and vertical directions. A pair of electrodes settled in the SFD to control the viscosity of lubricant was divided into a horizontal and vertical directions, and the directional controllability was investigated experimentally.

2. Liquid Crystal

LC is an organic liquid characterized by the long-range order of its molecular orientation (de Gennes, 1975 ; Okano and Kobayashi, 1985). This molecular orientation changes in either of two ways, in a certain range of concentration and in a certain range of temperature, resulting in two types of LC referred to as lyotropic and thermotropic, respectively. LC is also classified into high and low molecular-weight types. A finer classification is made on the basis of the structure of the molecular orientation. As shown in Fig. 1, four typical structural phases are known, nematic, smectic, cholesteric and discotic.

As a typical structure of LC, p-methoxy benzylidene-p'-butylanline (MBBA) is shown in Fig. 2. This is a low molecular-weight LC which emerges in the nematic phase in a temperature range between 22°C and 47°C. Since the temperature range for a LC phase of a single compound is not so wide, various kinds of LCs are mixed to expand the temperature range for practical use. As will be explained later, the sample LC used in the present experiment is a mixture of more than twenty kinds of LC.

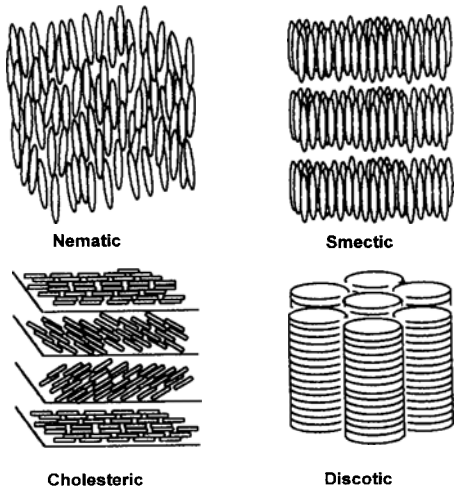

Fig. 1 Molecular model of liquid crystals.

The isotropic shape and particular structure of LC molecules generate some directional properties that appear, for example, as optical and electrical anisotropy, which causes their characteristic response to an external electric or magnetic field. The molecules of LC in the nematic phase generally have a long, cylindrical and ellipsoidal shape, the major axis of which can be controlled by an external electric or magnetic field. The unit vector, the direction of which is parallel to the major axis of the ellipsoidal body, is defined as the director. When an external electric field is applied, the dielectric anisotropy of LC, which is defined as the subtraction of the dielectric constant parallel to the major axis from that perpendicular to the axis, is one of the most important properties.

The viscosity of nematic LC is known to be anisotropic, and three limiting viscosities, called Miesowicz viscosities, have been defined for the three typical orientations of LC molecules in relation to the shear flow, as shown in Fig. 3 (Benicewicz, Johnson and Shaw, 1981). In Fig. 3, η_1: director is normal to the shear plane, η_2: director is parallel to the flow direction, η_3 : director is parallel to the velocity gradient.

Figure 4 shows the Miesowicz viscosities (Ga-

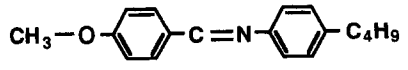

Fig. 2 Example structure of liquid crystal: MBBA.

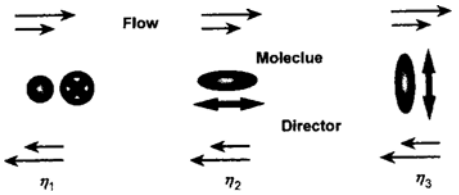

Fig. 3 The viscosity coefficients of nematic liquid crystal.

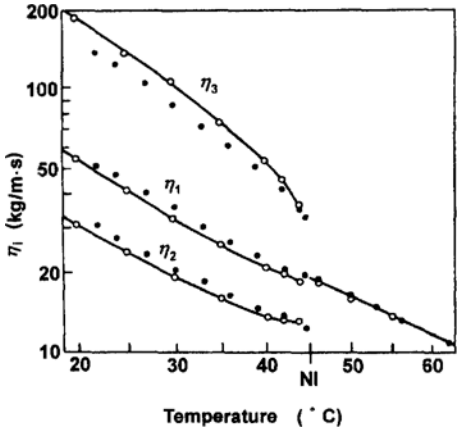

Fig. 4 Miesowicz viscosities in nematic liquid crystal.

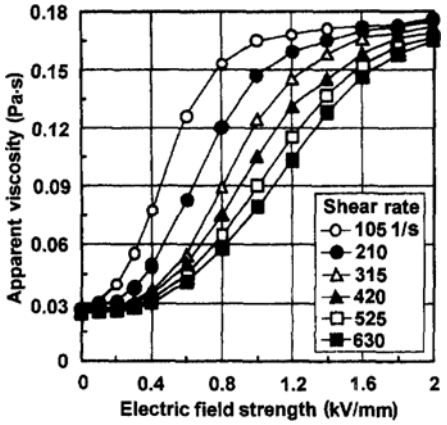

Fig. 5 Electroviscosity of liquid crystal.

Table 1 Properties of test sample.

Clearing point	100. 3°C
Resistivity	$1.2\times10^{11}\,\Omega$ · cm
Viscosity [20°C]	0.0415 Pa · s
Ordinary axis	1.499
Refractive anisotropy	0.146
Dielectric constant	16.3
Dielectric anisotropy	11.3

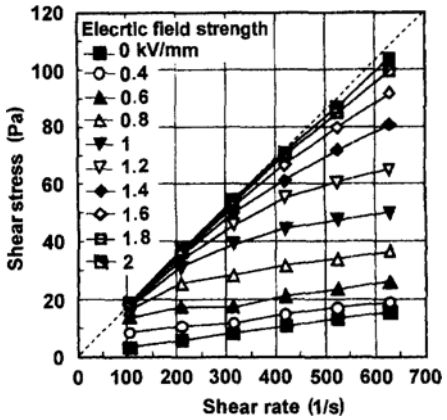

Fig. 6 Shear stress versus shear rate for liquid crystal.

hwiller, 1973) generally increase in the order $\eta_2 < \eta_1 < \eta_3$. When the director of the molecules is controlled by an applied electric field, the viscosity may vary from η_2 to η_3.

3. Experiment

3.1 Test sample

The sample LC is a mixture of thermotropic low molecular-weight LCs, the main component of which is biphenyls. It has been originally developed for computer display devices, and shows the nematic phase between the temperatures of the clearing point and the melting point. The main properties are shown in Table 1.

3.2 Electroviscosity

Figure 5 shows the variation of apparent viscosity measured by a rotational viscometer under electric field strength at the temperature of 30°C. The apparent viscosity begins to increase rapidly in accordance with the increment of the applied electric field strength. The apparent viscosity is higher at lower shear rates, but not so much remarkable at high shear rates. When the electric field strength comes up to a certain level, the gradient of apparent viscosity increases gradually and approaches a constant value regardless of the shear rates. Therefore, although higher electric field applied, the viscosity has essentially a constant value in the case of high shear rates. DC field was used as the applied electric field.

Figure 6 is an alternative representation of Fig. 5. Gradients of each line indicates the Newtonian viscosity. It is shown that the properties resemble

that of the pseudoplastic fluid at lower electric field strength, and the gradient increases and approaches a certain value at higher electric field strength. Because the rotational viscometer generates one directional shear flow, the properties measured by the rotational viscometer would not be realized in the SFD. Appreciation of the viscosity in itself requires measurement of viscosity in a reciprocating-type viscometer. However, the electroviscous effect is estimated by the traditional rotational viscometer in this study.

3.3 Controllable squeeze film damper

Figure 7 shows the experimental apparatus. A flexible shaft with three flywheels is supported by ball bearing at both ends, and one end is connected to a variable-speed motor through a flexible coupling. For simplicity, the controllable SFD is only mounted around the outer ring of the ball bearing at the opposite side of the shaft connected to the motor. In the opposite side a conventional SFD is used and the detailed construction of the controllable SFD is shown in Fig. 8. A pair of electrodes are installed inside of the SFD using LC. The whirling orbit of a flexible shaft is generally not a circular one but an ellipsoid. The whirling amplitude of the shaft at each

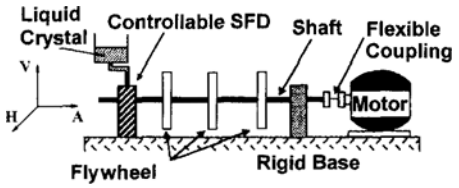

Fig. 7 Experimental apparatus.

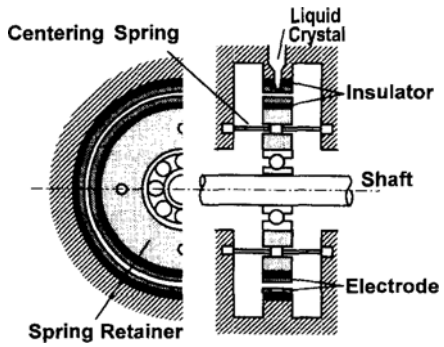

Fig. 8 Construction of squeeze film damper.

rotating speed can be effectively minimized by controlling the damping forces directionally. The inner side electrode is connected to a center spring retainer and the outer electrode is set up in the damper housing. Both electrodes were insulated by fiber reinforced composite material ring. In order to get the directional damping, the pair of electrodes were divided into two pair of electrodes in the vertical and horizontal directions.

The ball bearing with center spring retainer is supported by several centering pin springs and the retainer was hung up by piano wire on a low stiffness coil spring. The supporting stiffness can be altered by varying the number of supporting pin springs. In this experiment, four pin springs is used and the principal dimensions are shown in Table 2.

In the experiment, the rotor was not driven but excited by giving an impact to a side flywheel close to the controllable SFD. Moreover, impulse responses of free vibration and mode shapes of the rotor were measured with changing the applied voltage to the controllable SFD by several eddy current sensors set along the shaft. The natural frequency and equivalent damping ratios were estimated from the impulse responses under each electric field strength, which causes supporting stiffness variations. All the experiments were conducted at 30℃ by blowing hot air to the damper housing, because the properties of the LC is dependent on the temperature.

4. Results and Discussions

Figure 9 shows typical damped oscillatory

Table 2 Principal dimensions.

Rotor length	700 mm
Shaft diameter	20 mm
Rotating speed	500~4500 rpm
Damper diameter	72 mm
Radial clearance	0.1 mm
Damper width	10 mm
Oil groove width	4 mm

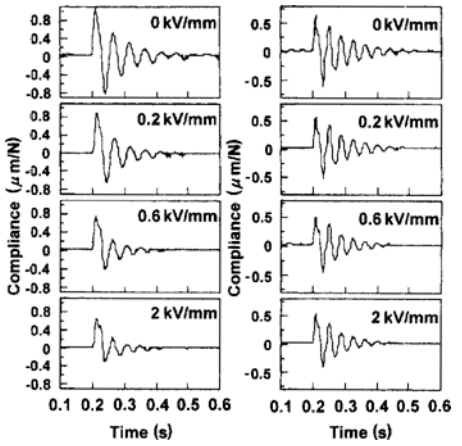

(a) Horizontal direction (b) Vertical direction

Fig. 9 Impulse responses.

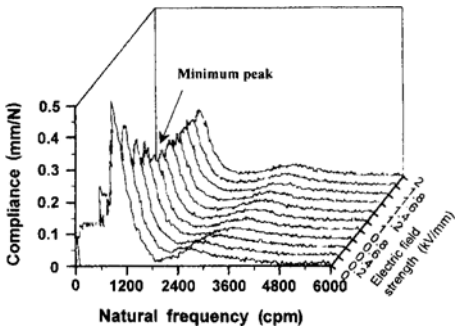

Fig. 10 Spectrum of impulse response in horizontal direction.

motion of responses to an impact under various electric field strength. The impulse responses in the horizontal and vertical directions are obtained when electric field is applied in the same direction. As the damping is increased by strengthening the electric field strength, the response amplitude is diminished. Moreover, the period of the horizontal direction is getting shorter but that of the vertical direction is not. When the electric field strength applied is over 0.6 kV/mm, there is no further change in responses due to the electric field increases.

Transfer functions of horizontal and vertical directions under various electric field strengths are shown in Figs. 10 and 11, respectively. The first and the second natural frequencies of the horizontal direction in Fig. 10 are about 1200 cpm and 2610 cpm, respectirely without electric

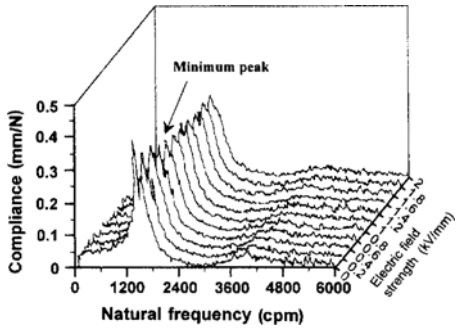

Fig. 11 Spectrum of impulse response in vertical direction.

field. Paying attention to the peaks corresponding to the first and second natural frequency, we can note that the peaks reduce gradually as the electric field strength increases. The peaks of the first natural frequency at 0.8 kV/mm and second natural frequency at 0.6 kV/mm are minimum height in Fig. 10 and this electric field strength applied in the SFD produced optimal damping in the rotor system. When the applied electric field is strengthened further, the peaks begin to increase after the damping have reached the optimum. During this transition, the first natural frequency elevated from 1200 cpm to 1380 cpm , the second from 2610 cpm to 3540 cpm.

In the vertical directions, the first and the second natural frequencies are about 1590 cpm and 3930 cpm without electric field. Note that those peaks corresponding to the first and second natural frequencies decrease gradually as the electric field strength is increased. Simultaneously, the second natural frequency elevated from 3930 cpm to 4080 cpm but the first natural frequency is not changed. These phenomena possibly depend on the variation of the supporting damping force. Because the viscosity of the LC can not be varied greatly with the applied electric field strength, the supporting condition can not be changed dramatically.

The changes of both peaks and natural frequency might be caused by mode shape variation due to the supporting damping force change produced by the controllable SFD. When the electric field strength is increased, the supporting damping become greater and the supporting con-

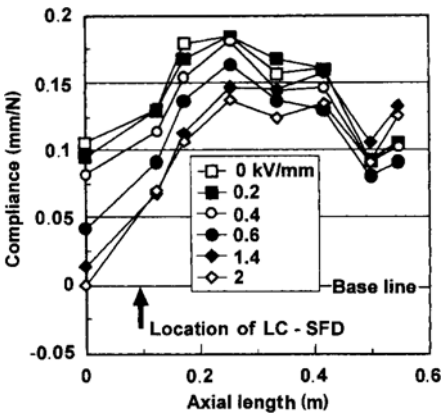

Fig. 12 Rotor mode shape in horizontal direction.

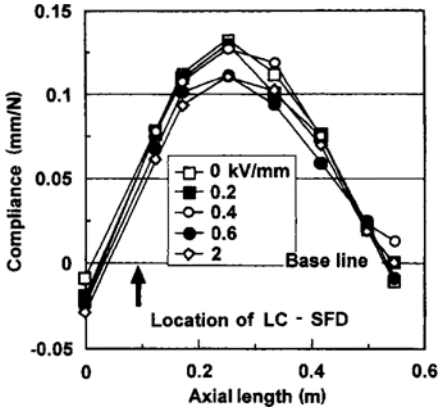

Fig. 13 Rotor mode shape in vertical direction.

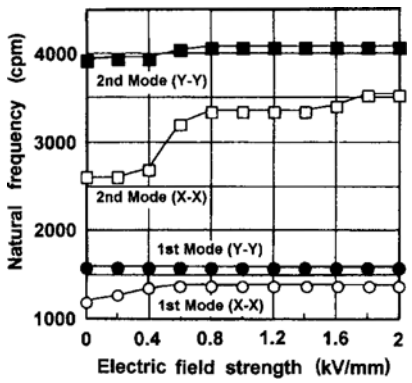

Fig. 14 Influence of electric field on natural frequency.

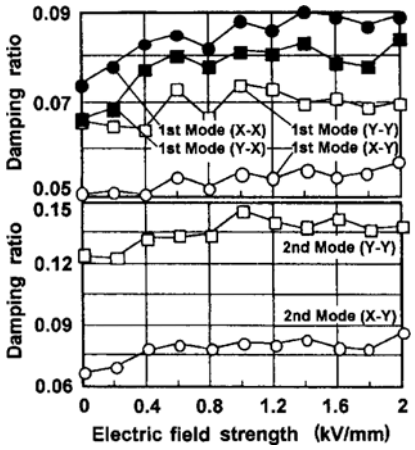

Fig. 15 Influence of electric field on damping ratio.

dition came close to simply-supported (Morishita and Mitsui, 1992).

Figures 12 and 13 show the mode shape around the first natural frequency in the horizontal and vertical planes, respectively. When the shaft is in equilibrium, it stops at the position of base line. When the electric field is increased, the oscillating amplitudes at the supporting point by the controllable SFD become small, which shows the change of the boundary condition with the variation of the supporting damping.

The variation of the natural frequencies described above is rearranged in Fig. 14 and the equivalent damping ratio in Fig. 15. Both the natural frequency and the equivalent damping ratio were estimated from the peak values of the spectrum in Figs. 10 and 11. When the applied electric field is strengthened, the first and second natural frequencies of the horizontal direction are increased gradually. However, the second natural frequency in the vertical direction increases a little, but the first natural frequency is not changed. (X-X) and (X-Y) are response of the horizontal, and vertical directions respectively, when an electric field is applied to the horizontal direction. (Y-Y) and (Y-X) are responses of the vertical, and horizontal directions, respectively when an electric field is applied to the vertical direction.

Because the S/N ratio is so small in the experiment, the damping ratio and the electric field strength of optimum damping are not identified exactly. However, the damping ratio is increased by strengthening electric field strength.

5. Conclusions

In the present paper, LC is applied to the directionally controllable SFD for reduction of whirling amplitude of a flexible rotor in the wide range of its rotating speed. The conclusions obtained are as follows:

(1) The liquid crystal is successfully applied to the SFD for the stabilization of rotating system and the damping force can be controlled by the externally applied electric field.

(2) The damping forces can be supplied independently to the horizontal and vertical direction of the squeeze film damper, in which a pair of electrodes is divided into horizontal and vertical directions.

(3) The directionally controllable SFD can supply a different supporting optimum damping in the vertical and horizontal directions independently.

References

Benicewicz, B. C., Johnsonm J. F. and Shaw, M. T., 1981, "Viscosity Behavior of Liquid Crystals," *Molecular Crystals and Liquid Crystal,* Vol. 65, pp. 111~132.

Cognard, J., 1990, "Lubrication with Liquid Crystals," *Proceedings of American Chemical Society Symposium on Tribology and Liquid Crystaline State,* No. 441, pp 1~47.

de Gennes, P. G., 1975, "The Physics of Liquid Crystals," *Oxford University Press,* London.

Fischer, T. E., Bhattacharya, S., Salher, R., Lauer, J. L., and Ahn, Y., 1988, "Lubrication by a Smectic Liquid Crystals," *Tribology Transactions,* Vol. 31, No. 4, pp. 442~448.

Gahwiller, C. H., 1973, "Molecular Crystals and Liquid Crystals," Vol. 20, pp. 953~960.

Honda, T., Kurosawa, K. and Sasada, T., 1979, wkElectroviscous Effect in Liquid Crystals, " *Japanese Journal of Applied Physics,* Vol. 18, No. 5, pp. 1015~1018.

Miesowicz, M., 1946, Nature, Vol. 158, pp. 27~37.

Morishita, S., 1995., "Controllable Damper Using Liquid Crystal," *Transactions of the JSME Part C,* Vol. 61, No. 581, pp. 43-48.

Morishita, S. and Mitsui, J., 1992, "Controllable Squeeze Film Damper (An Application of Electro-Rheological Fluid)," *Transactions of the ASME, Journal of Vibration and Acoustics,* Vol. 114, No. 3, pp. 354~357.

Morishita, S., Nakano, K. and Kimura, Y., 1993, "Electroviscous Effect of Nematic Liquid Crystals," *Tribology International,* Vol. 26, No. 6, pp. 399~403.

Morishita, S. and Ura, T., 1993, "ER Fluid Applications to Vibration Control Devices and an Adaptive Neuro-Net Controller," *Journal of Intelligent Material Systems and Structures,* Vol. 4, July, pp. 366~372.

Okano, L. and Kobayashi, S., 1985, "Liquid Crystals," *Baifukan.*

Satio, S., Someya, T. and Azuma, T., 1982, "On the Vibration of a Rotor Supported by Squeeze Film Damper," *Transactions of the JSME,* Vol. 48, No. 436, pp. 1883~1888

Ticky, J. A. and Rhim, Y., 1989, "A Theory for the Lubrication of Layered Liquid Crystals," *Transactions of the ASME, Journal of Tribology,* Vol. 111, No. 1, p. 169~173.